



Study the Phonocardiography

<i>Ali Karim Shaniour Obaid</i>	<i>Madent Alelem University College Medical physics ali1941999473@gmail.com</i>
<i>Hassan Nasser Diwan Nasser</i>	<i>Madenat Alelem University College Medical physics hassan96naser@gmail.com</i>
<i>Abdul Ilah Hassoun Harbi</i>	<i>Al-Hilla University College Department of Medical Physics /abdulilahhason201@gmail.com</i>
<i>mustafa Hamza Shabeeb</i>	<i>future University college medical physics twfytwfy819@gmail.com</i>
<i>Abdul Rahman Kazem Obaid Odeh</i>	<i>Al-Hilla University College Applied medical physics bwdjbwry701@gmail.com</i>

ABSTRACT

This project Phonocardiography and analysis using standard deviation profile was complete in Dhaka, Bangladesh, October-2013 and the models were randomized to thirty cases. This project gives a brief idea on heart signal processing by using the method of phonocardiography. A digital stethoscope was used to pick up the heart sounds from different patients and the corresponding analysis was performed. The project mainly attempts the use of standard deviation profile in heart rate calculation instead of the existing shanon energy profile at noisy environments. The project also emphasizes on the heart signal analysis using cheap and simple hardware and highly sophisticated use of software. Considering the results, the SureShrink algorithm is seen to provide the best performance the LMS-ALE algorithm resulted in an HS recovery of 91- 93% with 89-92% noise reduction. RLS-ALE turned up 95-97% HS recovery with 90-92% noise reduction.

Keywords:

Phonocardiography, analysis , standard deviation. Dhaka

Introduction

In developing nations of the world there is often a shortage of medical specialists and limited access to diagnostic equipment which lead to a poor basic healthcare system. For example in Bangladesh, the number of physicians for every 1000 people is 0.3 while in the United States it is 2.4 (World Bank 2010). This problem is particularly eminent in rural areas and as a result people residing in such communities are forced to travel long distances from their home to seek medical attention in more urban areas. This travel can be financially burdensome, uncomfortable to the patient and includes risk of road accidents. In many cases, it might deplete a family's savings and leave them destitute. Lack of medical attention for patients in developing nations has fatal consequences. The most alarming statistics are in the case of cardiovascular diseases (CVDs). CVDs are the number one cause of death globally. According to the World Health Organization (WHO), an estimated 17.3 million people died from CVDs in 2008, representing 30% of all global deaths. Of these deaths, an estimated 7.3 million were due to coronary heart disease and 6.2 million were due to stroke. Low- and middle-income countries are disproportionately affected: over 80% of CVD deaths take place in low- and middle-income countries. The number of people who die from CVDs, mainly from heart disease and stroke, will increase to reach 23.3 million by 2030 and CVDs are projected to remain the single leading cause of death. This emphasizes the need for improved healthcare access for these people. An abnormal heart rate can often be an indicator of a CVD. The aim of this thesis is to develop an algorithm that can be used to calculate the heart rate of a patient. The device that used for detection of the heart sound is a modified stethoscope. The earpiece of the stethoscope is replaced with a microphone input jack. The sound

recorded by the stethoscope can then be fed into the signal processing software in a computer or a cell phone. For people in rural areas, the use of a cell phone and stethoscope to measure the heart rate would be very convenient. Before moving on to the signal processing part an overview of the heart and heart sounds is in order.

1.1 Physiology of the heart

The heart is made up of four chambers: the right and left ventricles, and the right and left atria. The right and left sides of the heart are separated by the septum. Circulatory blood flow proceeds through the following sequence: body circulation, vena cava, right atrium, right ventricle, pulmonary artery, lungs, pulmonary vein, left atrium, left ventricle, aorta, body circulation (see Figure below) In order for this flow to occur, the heart muscle contracts and relaxes in a repeated cycle, with the blood being forced to follow the correct pattern with the help of heart valves.

Initially, the atria collect the blood from the circulation or lungs, depending on the side of the heart, in a passive way. This is the filling stage of the cardiac cycle, and is called the diastole. During this period, the valves separating the atria and the ventricles are open; these are the right (mitral) and left (tricuspid) atrioventricular (AV) valves. The valves between the right ventricle and pulmonary artery (pulmonary valve) and the left ventricle and aorta (aortic valve) remain closed during the diastole. At the very end of the diastole, the atria contract, forcing more blood into the ventricles.

The depolarization of the cardiac cells which caused the contraction of the atria then reaches to the ventricles. When the ventricles contract, the AV valves close due to the pressure difference, and the blood is ejected through the aorta or

pulmonary artery. Upon completion of ventricular contraction, the ventricles begin to relax and the dropping pressure quickly goes below that of the aorta and pulmonary artery, at which time the aortic and pulmonary valves close.

Heart valves operate passively, acting as check valves to prevent back flow and take no active role in controlling the direction of flow. This design allows the timing of the cardiac cycle to be controlled by a single source which under normal conditions is the depolarization of the sinoatrial (SA) node. The SANode has its own timing sequence, and although the brain may modify its action, it is not under the direct control of the brain. This makes the heart a very independent organ.

The final discussion point regarding the physiology of the heart relates to the nature of pathological dysfunction. The heart valves may become calcified with deposits related to blood contents. Due to the passive nature of their operation, the resulting stiffening is clearly detrimental to the function of the valves and is therefore the factor of most concern when diagnosing the heart. The cardiac valves may become weakened by other factors, causing them to be unable to function appropriately in the high-pressure environment of the heart.

The first heart sound, S1 is associated with the closing of the mitral and tricuspid valves. The second heart sound, S2 is associated with the closing of the aortic and pulmonary valves. This is further subdivided into the aortic valve (A2) and pulmonary valve (P2) closures. The sounds are actually slightly separated since the pulmonary valve closes slightly after the aortic valve; this may become more pronounced in pathological situations.

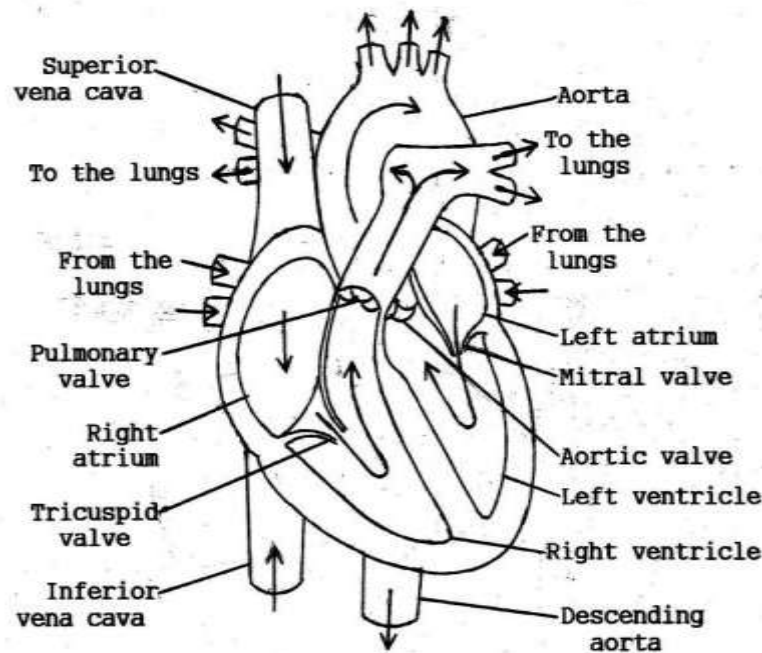


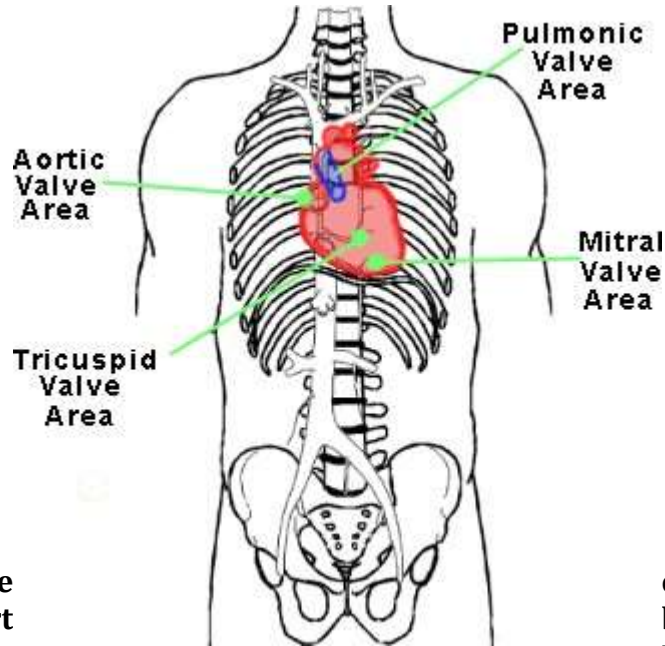
Fig: Structure of the Heart

1.2 Origins of Heart Sounds and Murmurs

There is wide agreement that normal heart sounds (S1 and S2) as heard by cardiac auscultation are not caused directly by the closing of the valves" but by vibrations set up in cardiac blood vessels by the sudden pressure change caused by the closing of the heart valves. As such, the amplitude of the heart sounds are expected to correspond with the size of pressure drop which in turn corresponds to the amount of fluid flow before valves closure. Also, the frequency characteristics correlate with the size of the valves, with lower frequency characteristics corresponding to larger valves. There has been much more debate regarding the origins of heart murmurs, likely as a result of the wide variety of physiological causes for the murmur themselves. However, studies have demonstrated that the origins of heart murmurs are the vibrations associated with turbulent flow. The sound energy density was also found to be proportional to the level of turbulence. Since laminar flow is the normal state of blood flow in human circulation, audible murmurs are usually associated with some pathological state. They are normally characterized by a higher frequency content than any other heart sounds⁴. Often heart murmurs do not indicate a pathological state. Any movement of fluid in a distensible chamber of vessel will cause vibrations of some sort, so everyone has some murmur if the recording instrument is sensitive enough

1.3 Recoding the heart sound

Cardiac sounds occur within a low frequency range. These can be classified into the categories discussed above. It is important to keep in mind that the audible presence of a certain class of heart sound can be normal for some ages but abnormal for others. For recording the signal, the stethoscope has to be placed on the chest and the output connected to a computer or cell phone. Amplitude is usually the loudest when the stethoscope is placed on either the tricuspid or mitral valve area.



The heart rate number of heart minute (bpm).

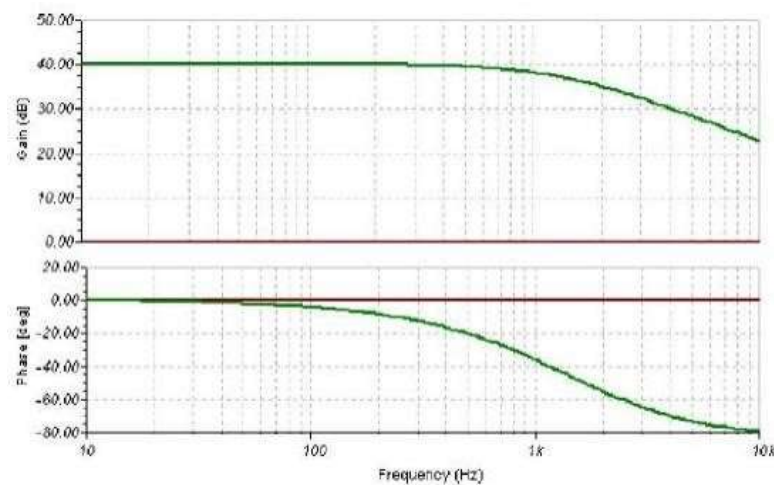
can be defined as the beats per minute. The range of acceptable heart rates for an average person at rest is claimed to be: 60 to 100 bpm for an adult, 50-100 bpm for a teenager, 74 to 140 bpm for a child and 70 to 170 bpm for an infant. Heart rates vary with age but other

factors such as fitness level, stress, exercise or any heart disease can also affect the heart rate.

2. Literature Review

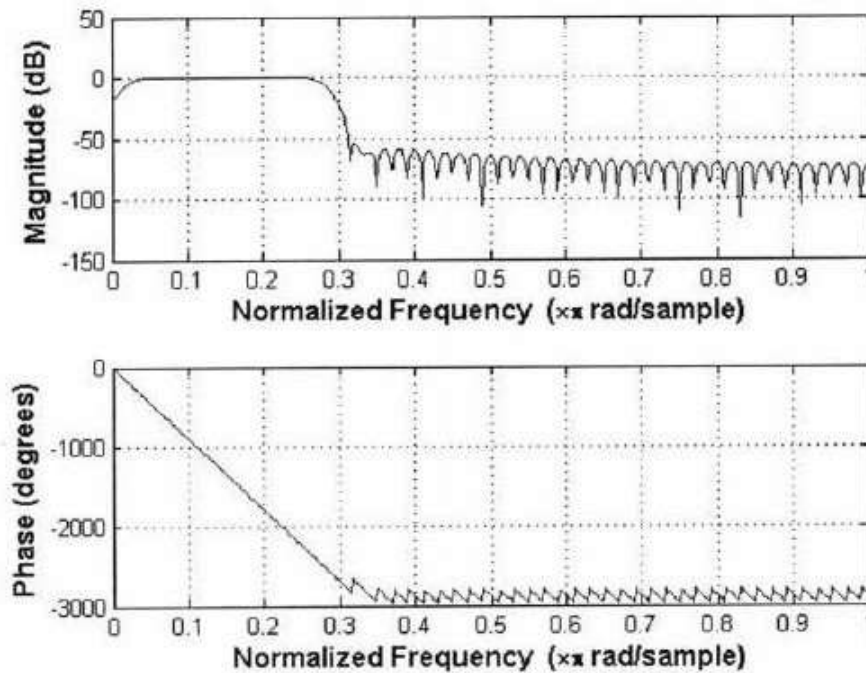
2.1 Heart sound signal retrieval and filtering

All heart sound signals were taken using an electronic stethoscope followed by the use of appropriate filters. In the paper by Liang *et al.* (1997), an eighth-order Chebyshev type-I low-pass filter was used with a cutoff frequency at 882Hz. The signal passed through the filter was originally sampled at 11025 Hz with 16-bit accuracy, but was decimated by a factor of 5 by the filter to result in 2205 Hz sampling frequency. The filtered signal was reversed and run back through the filter which results in zero phase distortion. In the paper by Fei Yu *et al.* (2008), a hardware low-pass filter was used to cut off high frequency components during recording. The frequency and phase response is as below.



Kumar *et al.* (2006), in their paper developed a procedure to first segment the heart sound signal into lobes with defined boundaries. Unlike the previously referred papers, Kumar avoided empirically tuning any filters. He performed the fast wavelet transform (FWT) using the db6 (Daubechies wavelet family) performed upto the 6th level to remove high frequency components. Daubechies wavelet family was used for its effectiveness in capturing transient sounds and the decomposition depth level of 6 was experimentally tuned.

In Kuan (2011) thesis the algorithm used by Pan and Tompkins in their paper (1985) used to determine the heart rate from ECG signals was carried over to do the same using an acoustic heart sound signal. After recording, the input signal is downsampled from 44.1kHz to 500Hz and normalized. The signal was then passed through a 100-point FIR bandpass filter with cutoff frequencies of 5Hz and 70Hz.

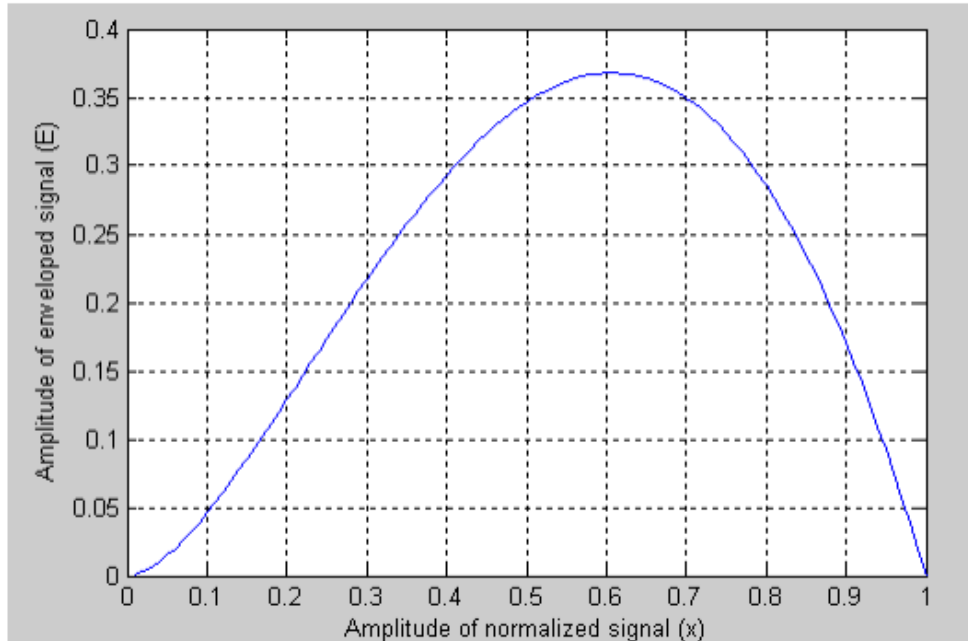


In the paper by Mandal *et al.* (2011), the retrieved heart sound was firstly preamplified before passing it through an LPF-HPF combination to remove unnecessary regions of the signal followed by post-amplification. It then goes on to highlight two different classes of filtering and denoising techniques. The first of these methods employ an adaptive line enhancer (ALE) using the least mean square (LMS) algorithm and also the recursive mean square (RMS) algorithm. The ALE is able to suppress wideband noise of the sound signal by utilisation of an adaptive filter (used as a linear prediction filter) with the reference signal being a delayed version of the input heart sound signal. The purpose of the delay is to decorrelate noise so as the adaptive filter is only able to predict the heart sound signal and not the noise. The output signal is then subtracted from the input signal to obtain the error signal which is used to adaptively control the filter weights and minimise error. The second method used wavelet-based denoising techniques. The orthogonal wavelet transform is able to compress the energy contained in a signal into a few large components with the disorderly noise characterized by small coefficients scattered throughout the transform. These smaller coefficients are omitted and the waveis reconstructed using the larger wavelet coefficients. Two orthogonal wavelet transform techniques are mentioned; one of them is SureShrink which is a smoothness adaptive algorithm and works at multiple levels of wavelet decomposition. It also estimates risks using Stain's unbiased risk estimator. The SureShrink algorithm's parameters were modified to expedite computation. The other technique, BayesShrink, though outclassed by newer techniques, was chosen for its efficiency in computation time which makes it viable for real- time operations.

2.2 Signal pre-processing

The signal is then processed further to help in the detection of the peaks. Liang *et al.* (1997) used a technique to help accentuate medium intensity signals over those of low and high intensities. This was achieved by normalizing the signal and determining the Shannon energy envelope of the signal.

$$\text{Shannon energy : } E = -x^2 \cdot \log x^2$$

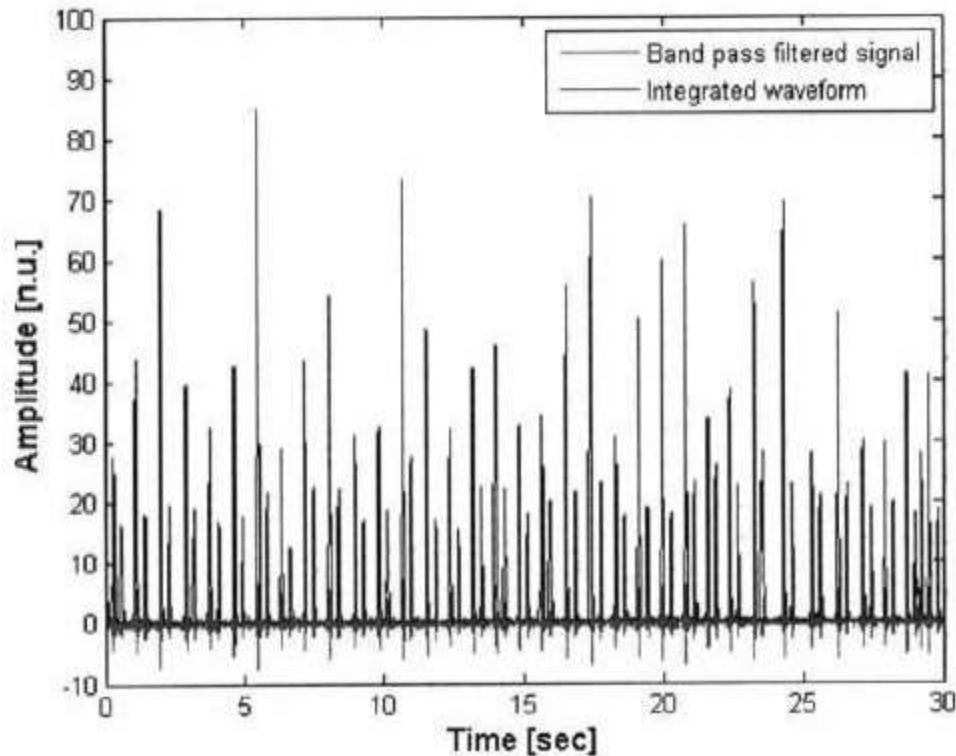


The average Shannon energy was calculated in continuous 0.02 second intervals with 0.01 second overlapping.

$$E_s = -\frac{1}{N} \cdot \sum_{i=1}^N x_{norm}^2(i) \cdot \log x_{norm}^2(i) \quad \text{where, } x_{norm} \text{ is the normalized and decimated signal.}$$

Fei Yu *et al.* (2008) manually extracted the peaks before subsequent processing. Details are given in the next section

Kuan and Katherine (2010) used the same technique employed by Pan and Tompkins. The energy of the heart sound signal was quantified by differentiating, squaring and integrating over an empirically determined window length of 58ms (or 29 samples long). The resulting integrated quantity peaked in high energy areas, i.e the S1/S2 sounds.



Kumar *et al.* (2006) using the signal approximation coefficients of the FWT he performed previously and the Shannon energy operator (given below), he computed the signal envelope.

$$E(x[n]) = -\frac{1}{N} \sum_{n=1}^N (x[n])^2 \cdot \log(x[n])^2$$

where, $X \in \{a_1, d_1, a_2, d_2, \dots, a_6, d_6\}$ and a_j, d_j are j th level approximation and detail coefficients of the wavelet transformed heart sound signal, respectively, and N is the number of samples in the selected window.

A window of 20ms was selected with 10ms overlaps to compute the Shannon energy. Boundaries of the sound lobes are identified out by analyzing the zerocrossing of the normalized Shannon energy,

$$E_n(a_5) = E(a_5) - \langle E(a_5) \rangle$$

where, ' $\langle \rangle$ ' represents the average operator and E_n the normalized Shannon energy. The 5th level approximation coefficients were used.

The lobe boundaries are validated by checking the sound lobe duration dt_i , the interval between two consecutive sound lobes T_i^{int} and their loudness measured as the root mean square of the segment RMS_i .

n_i^{start} and n_i^{stop} is the start and stop sample index of the i^{th} segment, respectively.

$$dt_i = T_s(n_i^{stop} - n_i^{start}) \quad \text{where, } T_s \text{ is the sampling period}$$

$$T_i^{int} = T_s \left(\frac{n_{i+1}^{start} - n_i^{stop}}{T_s} \right)$$

$$RMS_i = \sqrt{\frac{\sum_{j=n_i^{start}}^{n_i^{stop}} S(j)^2}{n_i^{stop} - n_i^{start}}}$$

where, $i = 1, 2, \dots$ segments,

And S is the heart sound signal

The conditions used for validation are stated below.

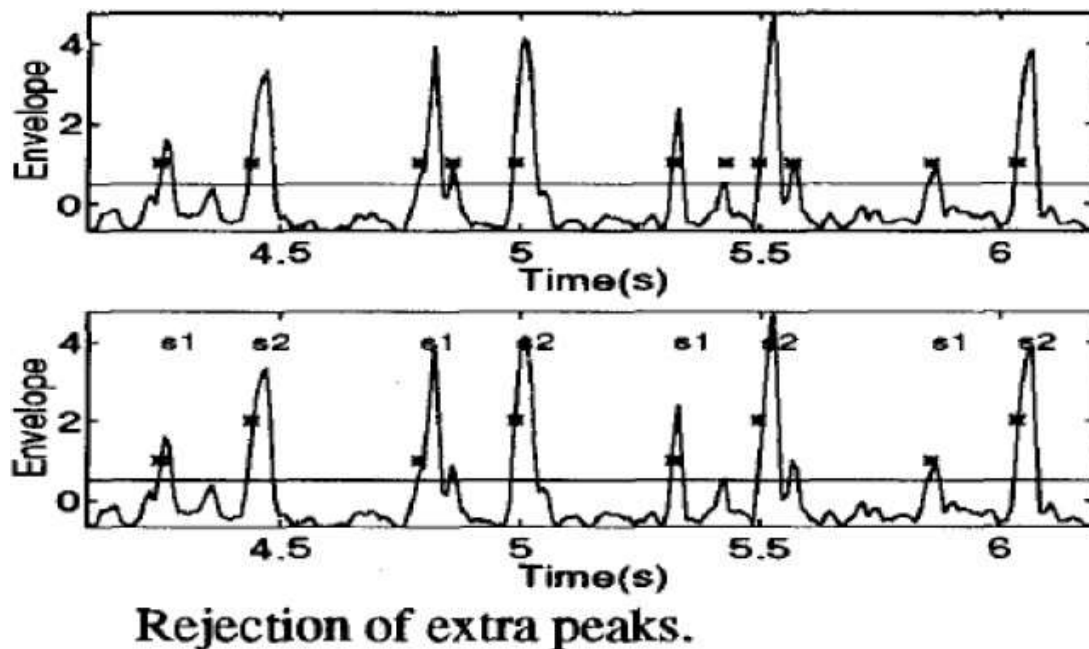
- i. If $dt_i < 30\text{ms}$ or $dt_i > 250\text{ms}$, the segment is considered to be noise-ridden and discarded. The durations were chosen on the basis of observed values in normal population.
- ii. If T_i^{int} is less than 50ms, the two segments are considered to belong to the same sound and the result of a split diastole. As the first segment (the aortic sound lobe) is more important than the second segment (the pulmonary sound lobe), the second is discarded.
- iii. Splitting might not be captured by the Shannon energy due to low loudness of low frequency sounds, but pronounced local minima is observed nonetheless. If the local minima is less than 25% of the maximum value of the Shannon energy, the splitting is considered to occur at that position and the part of the segment with the highest loudness is kept.
- iv. Sustained high frequency sounds may be mixed in with the recording like swallowing sounds, speech and abnormal valve closure among other disturbances. These noises are identified by computing jitter.

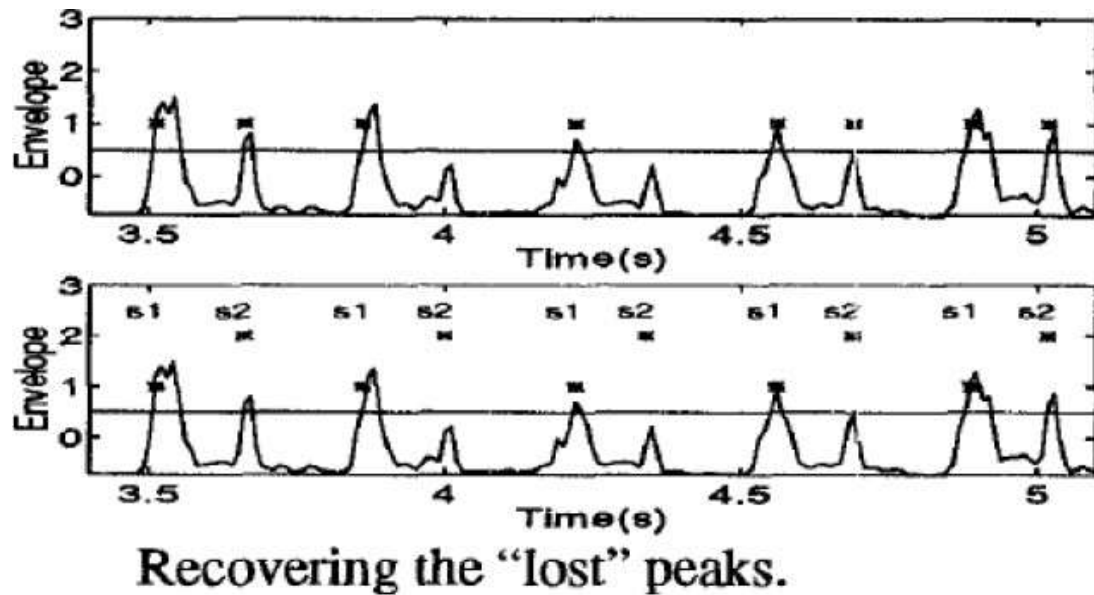
Mandal *et al.* (2011) performed decomposition of the signals upto level 5 by using Daubechies 6 (db6) wavelets. Levels 4, 5 and 6 detail coefficients were used to calculate the Shannon entropy after which the subbands were scaled and added up to give a partial reconstruction. The normalized Shannon energy signal envelope was computed and passed through a peak detector.

2.3 Peak detection and identification of S1 and S2s

The relevant peaks are then identified by introducing a threshold.

Liang *et al.* (1997) further delved into this process. Extra peaks were rejected by imposing a time-limit computed for each recording based on the mean interval and standard deviation. Any peaks occurring before the computed time was considered to be irrelevant, and disregarded. Similarly, an upper time-limit was used to search for any lost peaks. If none was found within that time, the threshold was lowered until one was picked up.





Then, to properly classify S1 and S2 sounds, Liang's algorithm took the largest interval between two peaks as the diastolic period and marked the successive intervals, both forwards and backwards, accordingly if they were within imposed tolerance values. Hence, S1s and S2s are also identified consequently with the start of the systolic period being S1 and the end being S2.

Kumar *et al.* (2006) utilized the fact that S2 sounds contain high frequency components that S1 sounds do not due to aortic valves closing with relatively higher pressure than mitral valves. In rare cases, like for patients using prosthetic single tilted disk valves, the S1 sounds are seen to contain the higher frequency components. Proper assignment of S1 and S2 is seen in the next section with this part discussing the determination of the location of the two sounds.

To extract the high frequency components of the segments identified previously, the Shannon energy operator is applied once more, but this time to

the segments and using the FWT detail coefficients. The adaptive threshold given below is used to make out the heart cycle,

$$th = E(d6) - \lambda < E(d6) > \quad \text{where, } \lambda \text{ is a constant initially fixed to 3.0}$$

and later adapted in certain situations

Applying this threshold, high-frequency segments (HFS) and low-frequency segments (LFS) can be detected in the segmented heart sound. A heart cycle can therefore be assumed to comprise of an LFS between two HFS with the duration between the two HFS being used to calculate the instantaneous heart rate. The duration is computed as follows,

$$T_{cycle}^k = \frac{dt_k}{2} + T_s(n_{k+1}^{stop} - n_k^{start}) + \frac{dt_k}{2} \quad \text{where, } T_{cycle}^k \text{ is the duration between } k^{\text{th}}$$

and $(k+1)^{\text{th}}$ HFS dt_k is the duration of HFS

Two conditions are imposed for the proper identification of heart cycles.

- i. If the heart cycle duration is greater than the average of the previous 3 durations, an HFS peak is assumed to have been missed. This is dealt with by lowering the HFS threshold by increasing λ in the adaptive threshold's algorithm by 0.1 intervals until the peak is found. The 3-cycle average is seen to be sufficient even in arrhythmic cases.

ii. If extra HFS markers are picked up due to noisy segments in the heart cycle, the correct one is identified by checking which peak was present in the previous cycle.

S1 and S2 sounds are classified by first estimating the systolic (S1-S2) interval duration from the cycle duration and comparing with every segment pair duration. The interval with the least deviation from the estimate is considered to be the S1-S2 interval with the starting segment designated as the S1 sound and the end segment, the S2 sound. In order to account for extreme arrhythmic cases which might render this classification process inefficient, the following steps are performed.

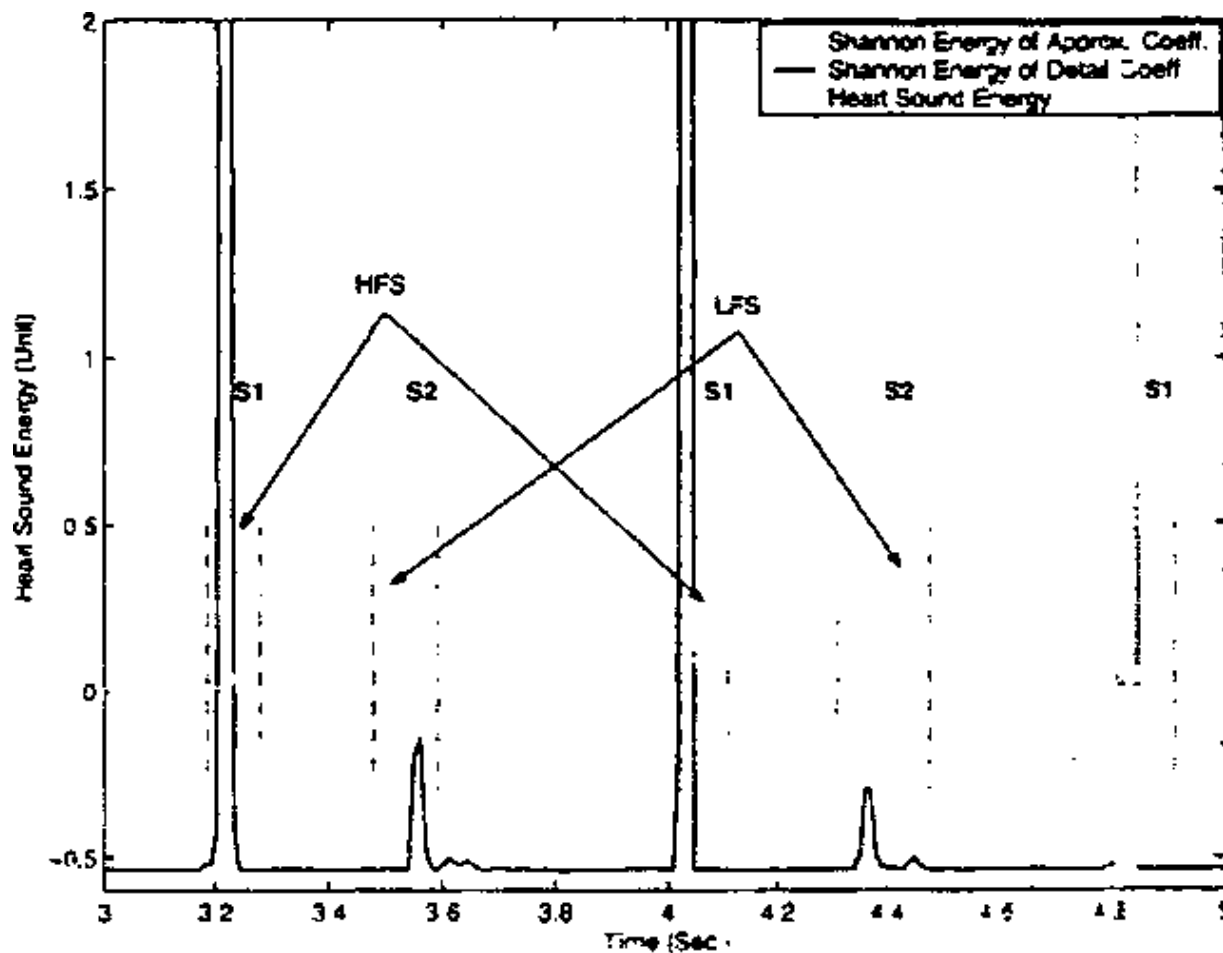
i. HFS cannot automatically be assigned to be S2 sounds in atypical cases, so proper identification of S1 and S2 sounds requires further checks to be performed. A correctly detected heart cycle is chosen containing 2 HFS and 1 LFS and the systolic interval is estimated from the cycle duration using the formula below,

$$T_{sys}^{est,k} = 0.2T_{cycle}^k + 160(ms) \quad \text{where, } T_{sys}^{est,k} \text{ is the estimated systolic interval}$$

of the k^{th} cycle

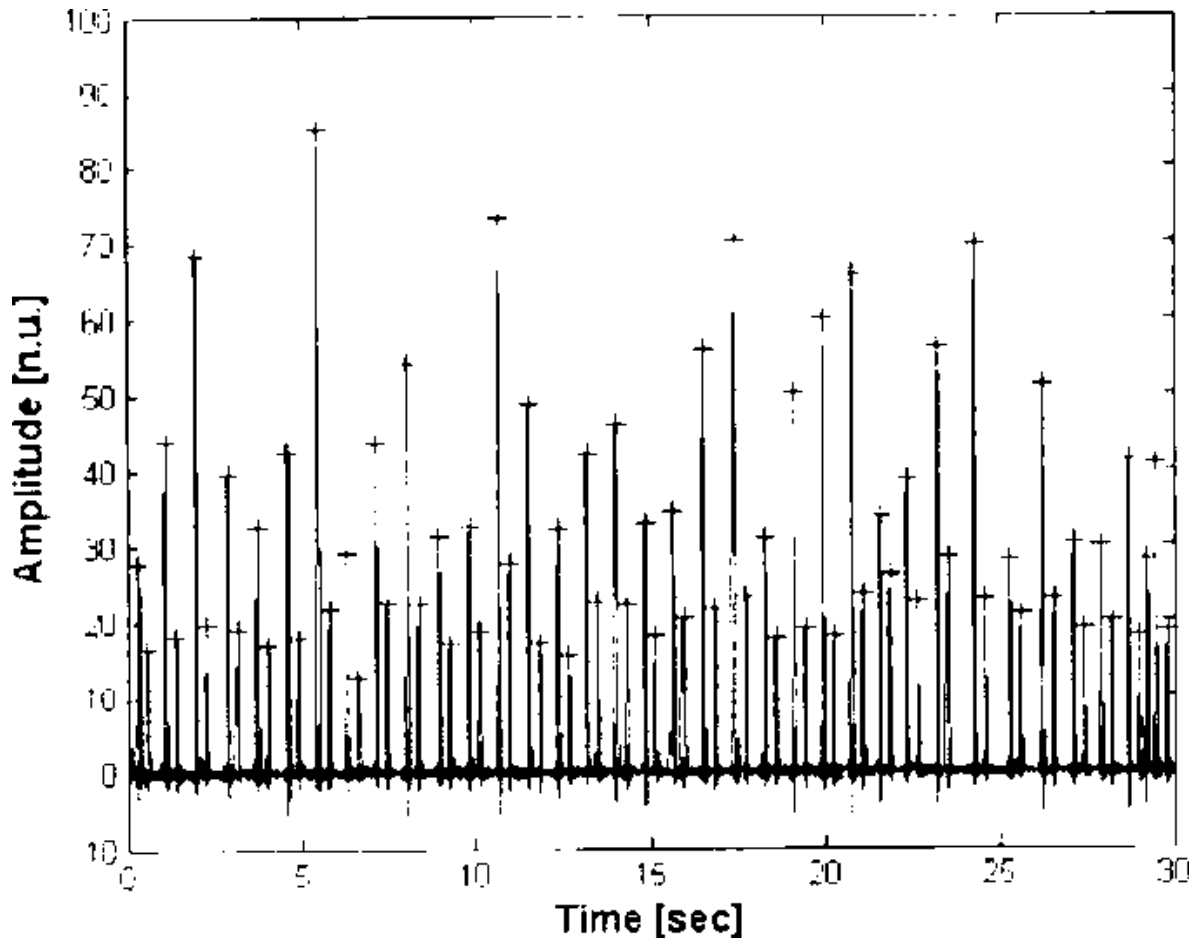
This estimated duration is compared to the two intervals (HFS-LFS and LFS- HFS) comprising the cycle and the interval with the smallest deviation from the estimated value is taken as the systolic interval. Hence, the starting segment class (either HFS or LFS) can be assigned as the S1 sound.

ii. The other segment class is assigned as the S2 sound.



Extraneous LFS segments might exist in the signal creating giving rise to more than one LFS segments between two HFS. The irrelevant LFSs can be removed by comparing the estimated systolic interval with all the possible LFS-HFS (or HFS-LFS, if HFS is assigned as S1) pair durations. The pair with the least deviation from the estimate is considered to be the correct LFS-HFS pair with all other LFSs making up the other pairs removed.

Kuan and Katherine (2010) did not discuss any methods used to properly pick up any missing peaks or eliminate extra peaks. She only used a threshold to pick up the peaks belonging to the S1/S2 sounds. After locating the peaks, intervals between the peaks were tabulated. This resulted in two Gaussian-like clusters. The intervals closer to the cluster with the smaller time period were considered the systolic periods and the other intervals, the diastolic periods with the relative peaks being assigned as S1 and S2 sounds.



Fei Yu *et al.* (2008) also used a simple threshold. He then manually isolated the two peaks and plotted their frequency spectrums to pick out distinguishing characteristics. It was observed that there are discernible differences between the two spectrums at the frequencies 15Hz and 65Hz. The S1 beat possesses

higher valued components at around 15Hz than the S2 beat and similarly, S2 contains components with greater amplitude at 65Hz than S1. Hence, a bandpass filter with cutoff frequencies at 10Hz and 20Hz was used to eliminate all S2 peaks from the signal leaving only the S1s. This signal was then normalized and the energy square calculated using the formula,

$$Y_{norm}(t) = \frac{[Y(t)]^2}{\max([Y(t)]^2)} \quad \text{where, Y is the amplitude of the signal}$$

The S1 peaks were evident when the above normalized signal was plotted against time. The peak locations can then be stored but to correct for the delay created by the filter the time value, taken to be T_{max} , S1 is assumed to start 0.26s earlier than T_{max} . The S1 peaks can be extracted and saved by taking out a 0.3s interval window from the plot starting from the acquired location. The same procedure was applied to find the S2 peak locations and the S2 extracted signal. Murmurs can also be isolated using the same algorithm.

The extracted signals can be convolved with the original signal to detect the quality, intensity and locations of S1s, S2s and murmurs. This can be used to monitor variation of the heart sound signal and perform diagnosis.

In the paper by Mandal *et al.* (2011) after passing the normalized Shannon entropy envelope through the peak detector, the subbands are again scaled and added up to give a partial reconstruction amplifying S1-S2 factors. Any peaks detected are sent to a boundary-calculation algorithm and adaptive thresholding is used to recalculate peak points in case none are detected. No further details of the algorithms were provided nor any mention of correctly distinguishing the S1 and S2 segments.

2.4 Heart rate calculation

Liang *et al.* (1997) did not delve into this section, their paper emphasized on the correct detection of peaks and their locations.

Fei Yu *et al.* (2008) computed energy square of the heart sound signal and passed it through a low-pass filter with a cutoff frequency of 10Hz. The resulting signal was then normalized and a threshold of 0.2 was used to correctly identify the peaks. Taking three of the peak locations, the heart rate was calculated as given below.

$$T = \frac{\Delta n}{f_s} = \frac{n_3 - n_1}{f_s} \quad \text{where, } f_s \text{ is the sample frequency, } n \text{ is the index, } \Delta n = n_3 -$$

n_1 is the number of samples in a heart beat cycle, and T is time period.

$$R_{hb} = \frac{60}{T} = \frac{60 f_s}{\Delta n} \quad \text{where, } R_{hb} \text{ is the heart beat rate}$$

Kuan and Katherine (2010) calculated the instantaneous rate by taking the median of the S1-S1 interval values over 9 beats around specified index peak

$$HR_i = \frac{60}{\text{median}(SS_{-4}, SS_{-3}, \dots, SS_3, SS_4)} \quad \text{where, } HR_i \text{ is the instantaneous}$$

heart beat rate at

i^{th} beat,

and, SS_i is the S1-S1 interval between beat i and $i + 1$

location.

Kumar *et al.* (2006) calculated the instantaneous heart rate previously (as detailed in the previous section) and used it for S1/S2 classification.

Mandal *et al.* (2011) did not include any mention of heart beat rate calculation in their paper.

2.5 Results

The algorithm developed was able to correctly identify peaks with about 93% accuracy and, tested under different conditions remained fairly robust in its efficiency. Misinterpretations were due to large background noises and serious murmurs (Liang *et al.*, 1997).

Fei Yu *et al.*, (2008) did not provide such specific numbers as their focus was primarily on the fabrication of an intelligent electronic stethoscope.

Kuan and Katherine (2010) used an ECG signal as a reference to test their system. The algorithm was able to correctly pick up peaks from the heart sound signal with 100% accuracy. It was also able to positively predict S1 peak locations with an accuracy of 88.4% and had a sensitivity of 92.1%.

Kumar *et al.* (2006) were able to achieve an average sensitivity of 97.95% and specificity of 98.20% testing on a range of patients possessing mechanical valves, bio-prosthetic valves and native valves. In the best case heart sound, 100% sensitivity and specificity was achieved and in the worst case sample, 95.67% sensitivity and 96.12% specificity. Wrong detection was mainly the cause of relevant adjacent segments being affected during removal of noise. The achieved sensitivity of noise detection by jitter approach was 92.20%, though high frequency noisy segments lasting less than 50ms were not able to be detected. A manual inspection of corresponding ECG signals' QRS complexes and T-waves was used as the reference.

Mandal *et al.* (2011) calculated the noise reduction and heart sound recovery percentages using the formulae below and compared the different filters and denoising techniques.

$$HS_{recover} = \frac{1 - E\{x_{HS}^2(n)\} - E\{y^2(n)\}}{E\{x_{HS}^2(n)\}} \times 100\%$$

$$NOISE_{reduction} = \frac{E\{x_{hsnoi}^2(n)\} - E\{y^2(n)\}}{E\{x_{hsnoi}^2(n)\}} \times 100\%$$

heart

where, $x_{HS}(n)$ is the original

sounds signal

and $x_{hsnoi}(n)$ is the one

corrupted with noise

The LMS-ALE algorithm resulted in an HS recovery of 91-93% with 89-92% noise reduction. RLS-ALE turned up 95-97% HS recovery with 90-92% noise reduction. Both BayesShrink and SureShrink algorithm recovered the heart segments with 96-98% accuracy with 88-91% noise reduction with BayesShrink and 91-92% noise reduction with SureShrink. Considering the above results, the SureShrink algorithm is seen to provide the best performance.

2.6 Conclusion

We observed that heart sound segmentation and peak extraction results were generally quite favourable but none of the papers delved into matters concerning environmental noise contamination of the recordings, the conditions under which the signals were taken and the effectiveness of their algorithms in non-ideal circumstances. Incorrect identification of peaks mostly occurred when faced with atypical heart signals indicating possible presence of cardiovascular diseases (CVDs). Carrying out diagnoses when dealing with such signals would prove more robust if compared with a database of heart sounds of patients with various CVDs. Hence, we conclude by highlighting that this field has room for more research and improvements which, if realized, could vastly help mitigating the increasing number of heart related deaths.

6-References

- [1] Liang, H.; Lukkarinen, S.; Hartimo, I., "Heart sound segmentation algorithm based on heart sound envelopogram," *Computers in Cardiology* 1997, vol., no., pp.105,108, 7-10 Sep 1997.
- [2] Fei Yu; Bilberg, A.; Voss, F., "The Development of an Intelligent Electronic Stethoscope," *Mechtronic and Embedded Systems and Applications*, 2008. MESA 2008. IEEE/ASME International Conference on , vol., no., pp.612,617, 12-15 Oct. 2008.
- [3] Kumar, D.; Carvalho, P.; Antunes, M.; Henriques, J.; Eugenio, L.; Schmidt, R.; Habetha, J., "Detection of S1 and S2 Heart Sounds by High Frequency Signatures," *Engineering in Medicine and Biology Society*, 2006. EMBS '06. 28th Annual International Conference of the IEEE , vol., no., pp.1410,1416, Aug. 30 2006-Sept. 3 2006.
- [4] Kuan, Katherine L., "A framework for automated heart and lung sound analysis using a mobile telemedicine platform", Thesis (M. Eng.)-- Massachusetts Institute of Technology, Dept. of Electrical Engineering and Computer Science, 2010.
- [5] Mandal, S.; Basak, K.; Mandana, K. M.; Ray, A.K.; Chatterjee, J.; Mahadevappa, M., "Development of Cardiac Prescreening Device for Rural Population Using Ultralow Power Embedded System," *Biomedical Engineering, IEEE Transactions on* , vol.58, no.3, pp.745,749, March 2011.
- [6] Gretzinger, David T.K., "Analysis of Heart Sounds and Murmurs", Thesis (M.Sc.)— University of Toronto, Institute of Biomedical Engineering, 1996.